Available online at www.sciencedirect.com
ScienceDirect
Journal of Photochemistry and Photobiology A: Chemistry 184 (2006) 26–33
Journal of Photochemistry and Photobiology A:Chemistry
www.elsevier.com/locate/jphotochem

Microwave electrodeless lamp photolytic degradation of acid orange 7

Xiwang Zhang *, Guoting Li, Yizhong Wang, Jiuhui Qu

State Key Laboratory of Environmental Aquatic Chemistry, Research Center for Eco-Environmental Sciences,
Chinese Academy of Sciences, P.O. Box 2871, Beijing 100085, China

Received 28 September 2005; received in revised form 6 March 2006; accepted 16 March 2006
Available online 30 March 2006

Abstract

Photolytic degradation of acid orange 7 (AO7) under microwave irradiation was investigated in which a novel microwave electrodeless lamp (MWL) was employed as light source. The novel MWL brings a new way to study the simultaneous effect of both UV–vis light and microwave irradiation on degradation of dye pollutants. Color, TOC, pH and inorganic ions concentrations with reaction time were monitored to evaluate the ability of MWL to degrade AO7. It was found that the coupled UV–vis/microwave irradiation led to excellent performance on decolorization and mineralization. AO7 solution could be completely decolorized at 80 min and mineralized at 150 min. Inorganic ions produced in the solution proved that AO7 was completely destroyed. The mechanism of MWL photolytic degradation of AO7 was investigated by examining the presence and role of some important oxidative species, such as superoxide ($O_2^{\bullet -}$), hydroxyl radical ($HO^\bullet$), H_2O_2 and O_3, using appropriate quenchers. The results showed that a large amount of H_2O_2 and O_3 could be generated in AO7 solution by MWL irradiation and the degradation of AO7 was mainly achieved by the attack of $HO^\bullet$ radicals resulted from photolysis of H_2O_2 and O_3. Direct oxidation of AO7 by O_3 and $O_2^{\bullet -}$ also played a few roles in degradation of AO7.

Keywords: Microwave electrodeless lamp (MWL); Acid orange 7 (AO7); Oxidative species; Mechanism

1. Introduction

Microwave is widely used domestically and industrially due to its heating effects on polar substances [1]. Other potential applications of microwave have been recognized and have been applied to a number of useful processes, such as organic and inorganic syntheses, polymerization, analyses and extraction, food sterilization, etc. [2–4]. Recently, microwave irradiation has been used to assist photochemical reactions for the degradation of organic pollutants [1,3–11]. Horikoshi et al. [3] proved that the integrated microwave/photocatalysis method was superior in the degradation of dye Rhodamine-B to TiO_2 photocatalytic degradative method alone. About 20% more $OH^\bullet$ radicals were found to be generated by photocatalysis with microwave irradiation than photocatalysis alone. Han et al. [5] showed that microwave irradiation could also considerably enhance the oxidative degradation of phenol in the H_2O_2/UV reacting system even under a suppression of the thermal effect.

Although microwave effectively accelerated photocatalytic or photochemical reaction as shown above, it is inconvenient for conventional electrode lamps to combine with microwave in photochemical reactions because their metal electrodes are easily damaged under microwave irradiation. The problem will be solved if microwave electrodeless lamp (MWL) substitutes the conventional lamp as light source because MWL has no electrodes. MWL comprises an envelope or bulb containing a plasma-forming medium. When it is placed in a microwave energy field the gases within the envelope will ionize, a low-pressure plasma discharge forms, heating and beating the envelope, vaporizing materials within the envelope to emit light. MWL brings a convenient way to study the synergetic effect of UV–vis irradiation and microwave irradiation on photochemical reactions. Comparative experiments in photoinitiated radical addition of tetrahydrofuran to perfluorohexylethene reaction showed that MWL provided a high yield of product in shorter reaction time [4]. Klán [12–14] also confirmed that MWL was feasible in light-induced photofragmentation reaction of valerophenone. More efficient photodegradation of Rhodamine-B and 2,4-dichlorophenoxyacetic acid were found in microwave assisted photocatalytic degradation with MWL (a double quartz

---

* Corresponding author. Tel.: +86 10 62849145; fax: +86 10 62923541.
E-mail address: xiwangzhang@126.com (X. Zhang).

1010-6030/$ – see front matter © 2006 Elsevier B.V. All rights reserved.
doi:10.1016/j.jphotochem.2006.03.021

cylindrical plasma photoreactor) as light source [6–8,10]. As illustrated above, MWL will be a prospective tool for microwave photochemistry including photodegradation of contaminants.

Dye pollutants, which are toxic to aquatic biota, can lead to aesthetic problem and eutrophication [15,16]. Most of the dyes are resistant to light. Even though under strong UV irradiation, what was found was slow decolorization or mineralization rate [17–21]. However, our researches [22,23] showed that the fast color removal of azo dyes Reactive Brilliant Red X-3B and acid orange 7 (AO7) under MWL irradiation were achieved. This indicated that the coupled UV–vis/microwave irradiation from MWL could accelerate the degradation of organic pollutants. However, the mechanism of photolytic degradation of organic pollutants under MWL irradiation has not been investigated in detail so far. In order to understand the synergetic effect of microwave irradiation and UV–vis irradiation further investigation was necessary.

In this study, AO7 was used as a typical organic pollutant to obtain detailed information of photolytic degradation of dye under MWL irradiation. The ability of MWL to degrade dye was evaluated by monitoring color, TOC, pH and some final inorganic products in solution. The degradation mechanism was also investigated by monitoring the formation and role of some oxidative species, such as H_2O_2, $O_2^{\bullet -}$ and $OH^{\bullet}$ radicals.

2. Experimental

2.1. Materials and analysis

The azo dye acid orange 7 was obtained from Beijing Xuanwu Chemistry Co., and used without further purification. The initial concentration of AO7 was 30 mg/L (86 μmol/L). Isopropanol (*i*-PrOH) and 1,4-benzoquinone (BQ), which were analytical grade, were purchased from Beijing Chemicals Co, in which BQ was purified by sublimation before used. Catalase (1870 units/mg) from bovine liver was purchased from Sigma Co.

The UV–vis spectra of the samples were recorded from 200 to 650 nm using a U-3010 UV–vis spectrophotometer (Hitachi Co., Japan). The concentration of the dye was determined by measuring the absorbance at a fixed wavelength (485 nm) according to the calibration curve established. Total organic carbon (TOC) in solution was measured by a Phoenix 8000 TOC analyzer (Tekmar-Dohrmann Co., USA). Determination of the concentrations of NO_2^-, NO_3^- and SO_4^{2-} ions in solution was accomplished by ion chromatography on a model 4500i (Dionex Corp.) The concentration of NH_4^+ ions in solution was measured by Nesslerization method. The pH of solution was measured by a model 828 pH meter (Orion Co.). The concentration of ozone in solution was measured by indigo colorimetric method. The concentration of hydrogen peroxide in solution formed during reaction was determined by a colorimetric method [24].

The formation of oxidative species, such as $O_2^{\bullet -}$, H_2O_2 and $OH^{\bullet}$ radicals, and their role in dye degradation process were investigated by means of appropriate quenchers of these species. Comparisons were made between the original decolorization curves of AO7 solution in MWL and those obtained after addition of quenchers in the initial solution, under otherwise identical conditions. BQ, *i*-PrOH and catalase were used as the quenchers of $O_2^{\bullet -}$, $OH^{\bullet}$ and H_2O_2, respectively. The dosages of BQ, *i*-PrOH and catalase were 0.01 mol/L, 0.01 mol/L and 500 mg/L with referring to other research, respectively [24–26].

2.2. Degradation procedures

The microwave source was a domestic microwave oven (Haier. Co. Ltd.; power, 700 W; frequency, 2.45 GHz). A cylindrical glass reactor (D: 10 cm; H: 15 cm) was employed all through the experiments. Air (0.15 m^3/h) was bubbled through a sintered glass filter fixed at the bottom of the reactor in order to mix the solution. The reactor was placed inside of the erect microwave oven as illustrated in Fig. 1. Solution temperature was kept at $38 \pm 1\,^{\circ}C$ by means of circulating solution to a cooler with a peristaltic pump. The whole system was filled with 750 mL AO7 solution, among which 125 mL was in the circulation pipe and 625 mL was in the reactor. MWL, which was made of quartz and filled with mercury and argon, was designed as U-shaped. The UV–vis spectra emitted by the MWL are depicted in Fig. 2. The MWL floated on the solution and about 60% was immerged in solution.

2.3. Estimation of the power of the MWL

The power of the MWL could not be measured directly just as conventional lamp. MWL emits UV–vis light by absorbing microwave energy. So, the power of MWL equals to the power of microwave absorbed by it. In this experiment, the power of microwave absorbed by the MWL could be measured by monitoring the temperature of solution and reactor. Microwave irradiation can linearly raise the temperature of the solution and reactor in the initial stage of reaction if the solution is not cooled by circulation. The temperature of the reactor is equal to the temperature of the solution in the reactor. Slope obtained from the straight lines can estimate the microwave power absorbed into the solution and reactor by a means of the following equation [5].

$$P = (c_w m_w + c_r m_r)\frac{\Delta T}{t} \tag{1}$$

where P is the power of microwave absorbed by solution and reactor (W), m_w and m_r masses of water and reactor (water: 750 g, reactor: 680 g), c_w and c_r the heat capacity of water and reactor (water: 4.184 J/g °C, reactor: 0.796 J/g °C), ΔT the temperature rise (°C) and t is the irradiation time (s). When the MWL is inside of the microwave oven and not immerged in water, the power (P_1) absorbed by water and reactor would be lower than the power (P_2) without the MWL in the microwave oven due to MWL absorbing partial microwave energy. P_1 and P_2 were 411.9 and 440.0 W in this system, respectively. It could be calculated that the power of MWL was 28.1 W. During reaction, the power of the MWL was less than 28.1 W because the power of microwave absorbed by the MWL was reduced because it was partially immerged in solution.

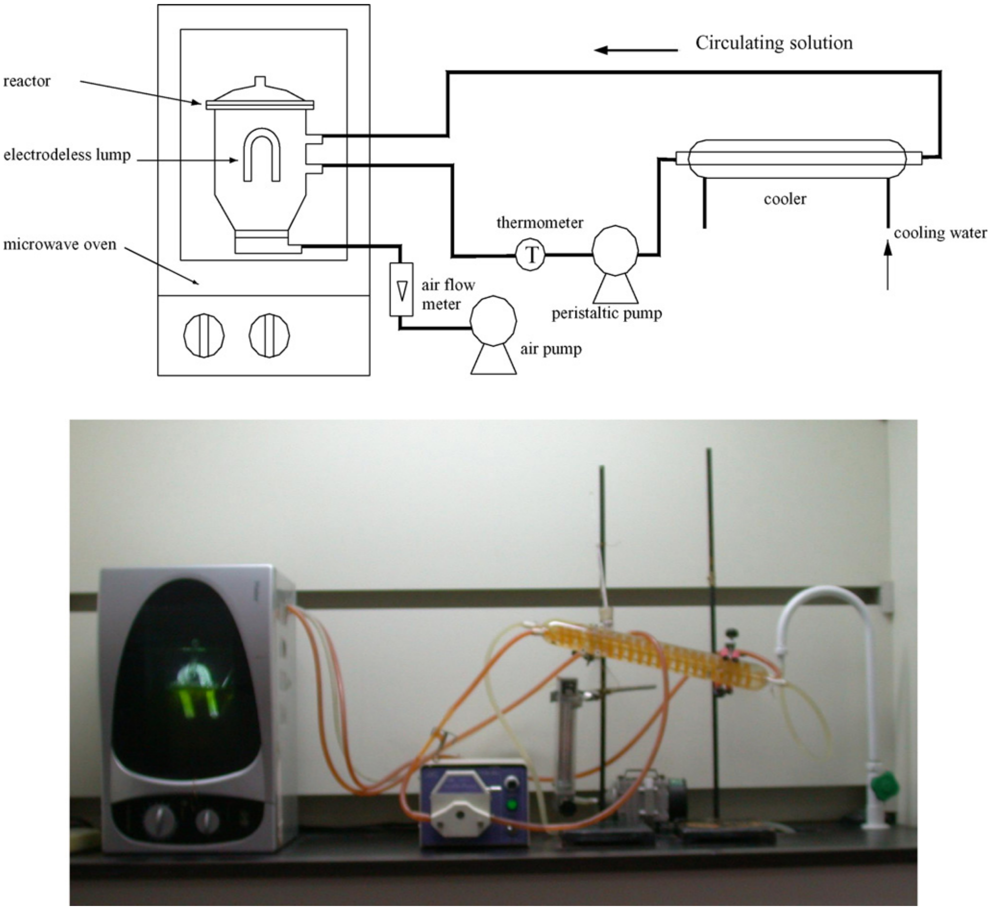

Fig. 1. Experimental setup for MWL photolytic degradation of AO7.

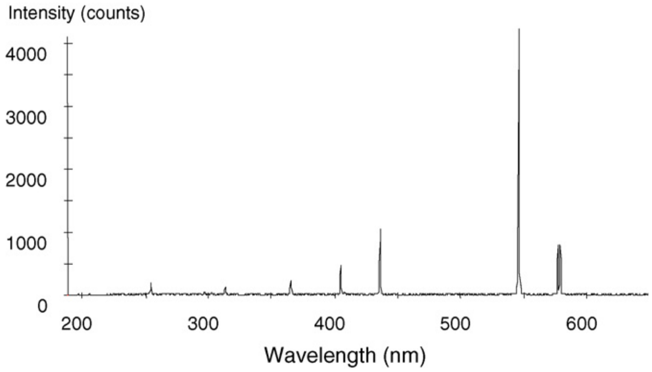

Fig. 2. Emission spectra of MWL.

3. Results and discussion

3.1. UV–vis spectral changes of AO7 solution with irradiation time

Fig. 3 shows typical UV–vis spectra obtained during MWL photolytic degradation of aqueous solutions of AO7. The spectrum obtained prior to MWL irradiation is characterized by two bands in the visible region, corresponding to the hydrazone form (485 nm) and azo form (430 nm) of the dye. These forms originate from intermolecular hydrogen bonding tautomeric interactions between the oxygen of the naphthyl group and the β-hydrogen of the corresponding azo-linkage, respectively [24]. The bands in the ultraviolet region, located at 310 and 228 nm, correspond to the naphthalene and benzene rings of AO7, respectively [24,27,28].

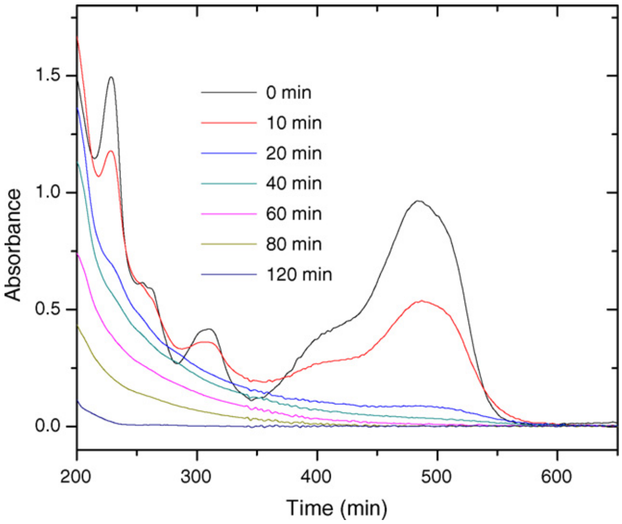

Fig. 3. UV–vis spectral changes of AO7 in solution under MWL irradiation as a function of time of irradiation.

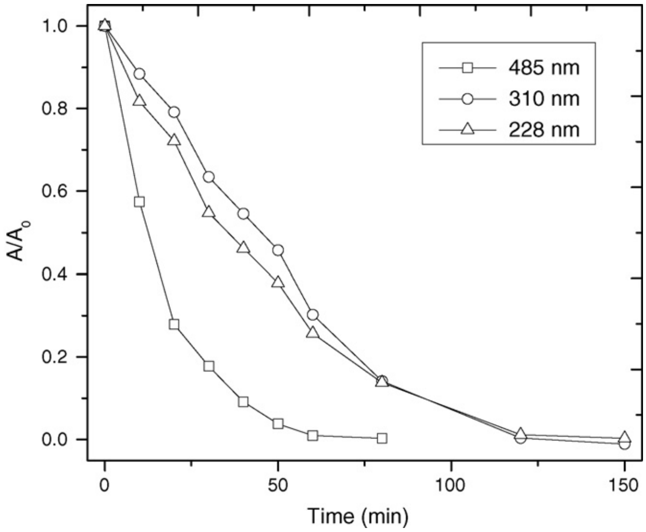

Fig. 4. Normalized absorbance of the main UV–vis bands of AO7 in solution as functions of time of irradiation.

It is observed that MWL has good performance on decolorization of AO7 from Fig. 3. MWL irradiation caused the absorption bands of the dye in the visible region to decrease with time and finally to disappear at 80 min, resulting in complete decolorization of the solution, which indicates the destruction of its chromophoric structure in the vicinity of the azo-linkage. This was accompanied by the decrease of the intensities of the bands in the ultraviolet region, located at 228 and 310 nm, as Fig. 4 illustrated. The UV–vis spectra of AO7 solution almost disappeared completely after 150 min. This indicates that the destruction of the naphthalene and benzene rings were achieved although it was slower than destruction of azo-linkage. No new absorption bands appeared either in the visible or in the ultraviolet spectral region. The relevant first-order kinetics of the transformation of AO7 at the three spectral wavelengths, 485, 310 and 228 nm, are 7.46×10^{-2}, 2.35×10^{-2} and $2.42 \times 10^{-2}\ \mathrm{min}^{-1}$, respectively. These data show that the cleavage of azo-linkage is about three-folds faster than these of benzoic and naphthalene rings.

3.2. Temporal change of pH

Fig. 5 shows temporal change of pH during MWL degradation in aqueous solutions of AO7. MWL irradiation caused significant decrease of pH in the period of the initial 100 min, from pH 6.15 at $t = 0$ to ca. pH 4.12 at $t = 100$ min. As has been shown in other study [24], the drop of pH with time was associated with the formation of acid products by the destruction of dye. However, further illuminating on the bleached solution caused an increase of pH up to 5.95 at the end of the experiment. This indicates that acid products were further degraded to small molecule substance, ultimately to CO_2. The pH of solution almost reached the initial value before illustration, which also indicates that the pH change of solution was resulted only from the formation of acid products.

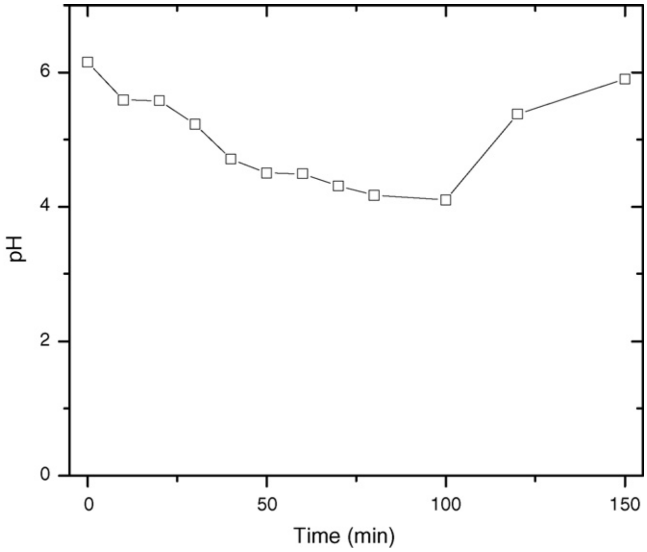

Fig. 5. Change of pH of the solution under MWL irradiation with time of irradiation.

3.3. Temporal change of total organic carbon

Total organic carbon value is the total concentration of organics in solution and the change of TOC mirrors the degree of mineralization as a function of irradiation time. Results of TOC measurements obtained during MWL irradiation treatment of aqueous solution of AO7 are presented in Fig. 6. It was observed that MWL irradiation had a good performance on mineralization. TOC was completely removed after 150 min irradiation. Obviously, the mineralization was divided into two stages as shown in Fig. 6. At the first stage (initial 60 min), the removal of TOC was very slow and less than 17% TOC was removed. It could be found from Fig. 4 that the color removal (485 nm) almost reached 100% at this stage. However, at the second stage (60–150 min) when the solution was completely discolored, the TOC removal

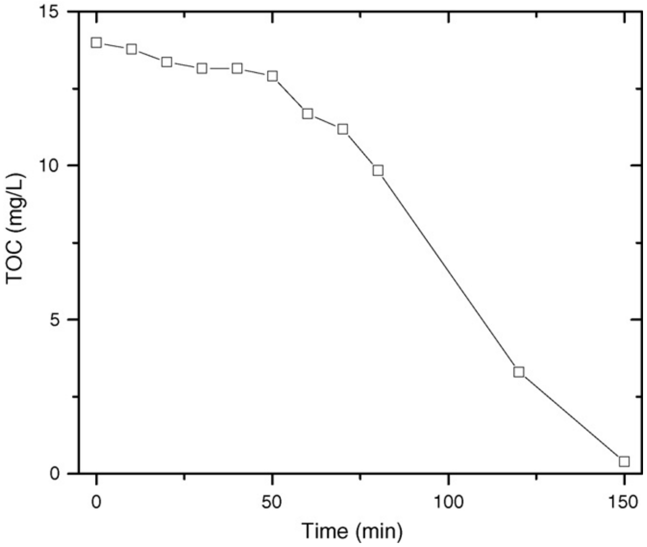

Fig. 6. Change of TOC of the solution under MWL irradiation as function of time of irradiation.

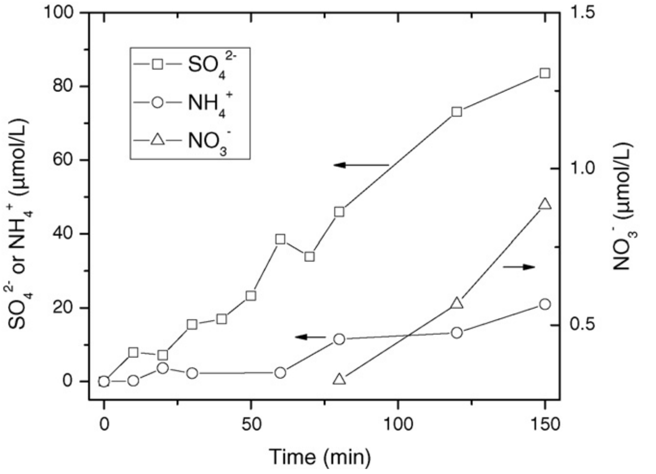

Fig. 7. Concentrations of inorganic ions in solution plotted as functions of time of irradiation.

accelerated remarkably. This phenomenon could be explained as following. At the first stage, most AO7 molecules were only destroyed to small intermediate substances. Subsequently at the second stage these small intermediate substances were further destroyed to CO_2 resulting in faster rate of TOC removal.

3.4. Formation of mineralization products

The evolution of inorganic ions in solution with time is shown in Fig. 7, where the concentrations of SO_4^{2-}, NH_4^+ and NO_3^- are plotted as functions of irradiation time. It was observed that the concentration of sulfate ions increased continuously and reached 83 μmol/L after 150 min irradiation. This quantity was almost the same as the expected (86 μmol/L) assuming complete mineralization of the dye, which indicates that all sulfonate groups were transformed to SO_4^{2-} under MWL irradiation.

As also observed in Fig. 7, a significant amount of NH_4^+ ions were produced from the initial stage. The formation of NH_4^+ was slow in the initial 60 min. When the solution was completely discolored after 60 min, the formation of NH_4^+ became fast to some extent. NO_3^- ions became detectable in solution after 80 min irradiation. Nitrate ion might be formed by oxidation of nitrite ion which, in turn, was formed by oxidation of ammonium ion [24,29]. In this experiment, NO_2^- was undetectable in the solution during reaction and the concentration of NO_3^- was 20 times lower than that of NH_4^+. This indicates that the formation of NO_3^- from NH_4^+ was very slow. At the end of the experiment, the sum of NH_4^+ and NO_3^- ions in solution was five times less than that expected from stoichiometry. It may be possible to assume that N_2 and/or NH_3 were produced and transferred into the gas phase.

Based on the results of above, it can be concluded that MWL photolytic degradation of dye can obtain complete decolorization and mineralization, which is deferent from conventional electrode lamp photolytic degradation. The photolytic degradation of dyes under UV–vis light irradiation alone can also achieve complete decolorization, but it is hardly to obtain mineralization [17–21]. Evidently, the difference of mineralization between MWL and conventional electrode lamp is caused by the synergetic effect of UV–vis irradiation and microwave irradiation provided by MWL.

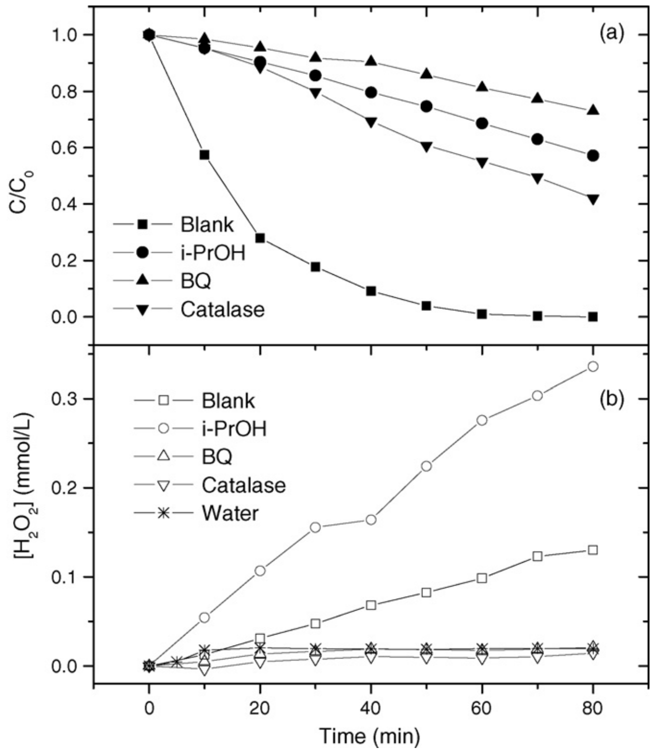

Fig. 8. Variation of normalized dye concentration (a) and H_2O_2 concentration (b) in solution in the presence of different quenchers.

3.5. Formation of oxidative intermediate species

i-PrOH is more easily oxidized by $HO^\bullet$ radicals. The rate constant of reaction between $HO^\bullet$ radical and *i*-PrOH is $1.9 \times 10^9\ M^{-1}\ s^{-1}$, a rate of almost the diffusion limit [25]. So it is usually used as diagnostic tool of $HO^\bullet$ radical. Fig. 8a shows the inhibitive effect of 0.01 mol/L *i*-PrOH on decolorization of the dye solution, under otherwise identical experimental conditions. It was observed that in the presence of *i*-PrOH, photobleaching of AO7 was suppressed. The apparent rate constant (k) of pseudo-first-order reaction decreased from 0.0746 to 0.0069 min^{-1}. The 90.8% decrease of k indicates that 90.8% decolorization of AO7 under MWL irradiation was achieved by $HO^\bullet$.

The hydrogen peroxide generated in AO7 solution without quencher under MWL irradiation is shown in Fig. 8b. It was observed that H_2O_2 was formed in the solution from the beginning of experiment and its concentration increased continuously with time. H_2O_2 acts as a precursor of many reactive species in light-driven reactions [30]. The role of H_2O_2 in dye degradation process has been investigated by means of catalase, a quencher of H_2O_2 [31,32]. A comparison was made between the original decolorization curves of AO7 solution and that obtained after addition of catalase (500 mg/L) in the initial solution. It was observed that decolorization rate decreased markedly and the k was 0.0104 min^{-1}, which decreased 86.1%. This indicated that H_2O_2 played an important role in MWL photolytic degradation of AO7. The decolorization of AO7 by the direct oxidation by H_2O_2 was negligible due to low reaction rate [20]. Evidently, other pathways rather than direct reaction with AO7 were involved for the degradation of AO7 by H_2O_2. As discussed above, $HO^\bullet$ was the main oxidative species leading to decolorization of AO7. Therefore, it was concluded that H_2O_2 took part in decolorization of AO7 by generation of $HO^\bullet$ as its precursor according to the following reaction [33,34]:

$$H_2O_2 + h\nu \rightarrow 2HO^\bullet \qquad (2)$$

Fig. 8 shows that the effect of addition of 0.01 mol/l BQ on the decolorization of dye solution and H_2O_2 generation. It was observed that in the presence of BQ, which is a $O_2^{\bullet -}$ quencher, both photobleching of AO7 and formation of H_2O_2 were suppressed. The k was only $0.0046\,\text{min}^{-1}$, which decreased by 93.8%. The amount of H_2O_2 in AO7 solution was largely less than that in the absence of BQ. This indicated that the superoxide radical was an important intermediate, which generated H_2O_2 and ultimately generated $HO^\bullet$. Cooper et al. [35] also proved that hydrogen peroxide appears to result from the disproportionation of $O_2^{\bullet -}$.

$$O_2^{\bullet -} + H^+ \rightarrow HO_2^\bullet \qquad (3)$$

$$HO_2^\bullet + O_2^{\bullet -} + H^+ \rightarrow H_2O_2 + O_2 \qquad (4)$$

$$HO_2^\bullet + e^- + H^+ \rightarrow H_2O_2 \qquad (5)$$

The formation of H_2O_2 in pure water under MWL irradiation was different from that in AO7 solution as shown in Fig. 8b. The concentration of H_2O_2 in pure water reached the maximal value (0.029 mmol/L) at 10 min and subsequently decreased slightly. However, 4.5 times higher concentration of H_2O_2 was observed in AO7 solution under MWL irradiation at 80 min with under otherwise identical conditions, reaching 0.13 mmol/L. It can be concluded that most H_2O_2 formed in AO7 solution under MWL irradiation were related to AO7. $O_2^{\bullet -}$, the precursor of H_2O_2, could be formed by the reduction of oxygen in solution where the light-absorbing substances (dissolved organic matter (DOM)) either generate free electrons by photoionization or reduce oxygen by energy transfer from the exited state [35,36].

$$DOM + h\nu \rightarrow DOM^* \qquad (6)$$

$$DOM^* \rightarrow DOM^{\bullet +} + e^- \qquad (7)$$

$$DOM^{\bullet +} + e^- \rightarrow DOM^{\bullet +} + e_{aq}^- \qquad (8)$$

$$DOM^* + h\nu \rightarrow DOM^{\bullet +} + e_{aq}^- \qquad (9)$$

$$e_{aq}^- + O_2 \rightarrow O_2^{\bullet -} \qquad (10)$$

It was proved that the dye molecules could be excited by visible light photons to produce singlet and/or triplet states [24,37]. Therefore, H_2O_2 could be generated by AO7 absorbing light according to the series of reactions as shown above. It was found that H_2O_2 did not disappear immediately when the solution was decolorized completely at 80 min. The concentration of H_2O_2 decreased gradually after 80 min and was close to the value in pure water when TOC was removed completely at 150 min (not shown). This implied that the intermediate products during degradation of AO7 also had the ability to generate H_2O_2 as light-absorbing substances. It was consistent with what was found by Cooper et al. [35] that many DOM in surface water and ground water could be exited by light to produce H_2O_2. The larger amount of H_2O_2 generated in the presence of isopropyl alcohol was also attributed to more DOM in the solution after addition of isopropyl alcohol.

As shown above, the k ($0.0069\,\text{min}^{-1}$) in the presence of $HO^\bullet$ quencher, *i*-PrOH, was lower than that ($0.0104\,\text{min}^{-1}$) in the presence of H_2O_2 quencher, catalase, indicating that there was other precursors of $HO^\bullet$ besides H_2O_2. It was doubtless that ozone was generated in the solution under MWL irradiation because odor of ozone was smelled during reaction. Ozone could be generated according the following reaction [36]:

$$O_2 + h\nu(< 242\,\text{nm}) \rightarrow 2O \qquad (11)$$

$$O + O_2 \rightarrow O_3 \qquad (12)$$

The concentration of ozone in solution after 30 min MWL irradiation was measured by indigo colorimetric method. Its concentration was 0.12 μmol/L. $HO^\bullet$ could be generated by the decomposition of ozone in solution by Eqs. (13) and (14) [38].

$$O_3 + h\nu(< 310\,\text{nm}) \rightarrow O^\bullet + O_2 \qquad (13)$$

$$O^\bullet + H_2O \rightarrow 2HO^\bullet \qquad (14)$$

According to (the) discussion above, the main pathway of oxidative species under MWL irradiation could be summarized as shown in Fig. 9.

The first-order apparent rate constants (k) of the decolorization in the presence of these quenchers are listed in Table 1. The contribution of $HO^\bullet$, H_2O_2 and $O_2^{\bullet -}$ to the decolorization of AO7 was 90.8, 86.1 and 93.8% according to their decrease percentages of k, respectively. The contribution of H_2O_2 was completely achieved by generating $HO^\bullet$ to oxidize AO7 because its direct oxidation was negligible as discussed above. That is, the contribution of $HO^\bullet$ resulted from H_2O_2 equaled that of H_2O_2 and was also 86.1%. It was presumed that other precur-

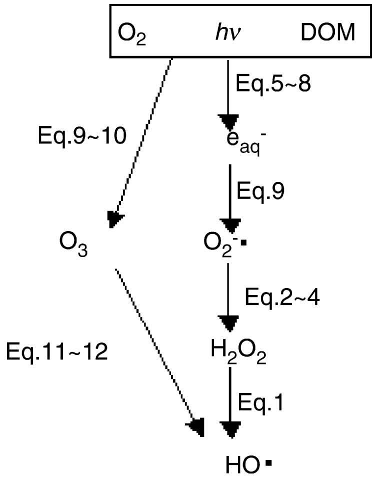

Fig. 9. Reaction pathways of oxidative species in AO7 solution under MWL irradiation.

Table 1
The first-order apparent rate constants (k) of the decolorization in the presence of *I*-PrOH, catalase and BQ

Quenchers	Blank	*i*-PrOH	Catalase	BQ
k (min^{-1})	0.0746	0.0069	0.0109	0.0046
Decrease percentage of k	–	90.8%	86.1%	93.8%

sors of $HO^\bullet$ were negligible besides H_2O_2 and O_3. Therefore, It could be calculated that the contribution of $HO^\bullet$ resulted from O_3 was 4.7% by subtracting the contribution of $HO^\bullet$ resulted from H_2O_2 from the total contribution of $HO^\bullet$. The contribution of H_2O_2 to the formation of $HO^\bullet$ was 18 times higher than that of O_3. However, the concentration of H_2O_2 was approximately 500 times higher than the concentration of O_3 at 30 min. Formation and decomposition of H_2O_2 and O_3 were simultaneous during reaction [31]. The reason why lower concentration of ozone was observed was that the decomposition rate of ozone was much higher than that of H_2O_2, approaching its formation rate. The molar extinction coefficient of ozone at 254 nm is 3300 $M^{-1}\ s^{-1}$, compared with 19.6 $M^{-1}\ s^{-1}$ of H_2O_2 [5].

The contribution (93.8%) of $O_2^{\bullet -}$ to decolorization was higher than that (86.1%) of H_2O_2, which indicated that 7.7% decolorization of AO7 was resulted from the effect of $O_2^{\bullet -}$ by other pathways rather than by forming H_2O_2. Although $O_2^{\bullet -}$ and its hydroperoxyl radical ($HO_2^{\bullet -}$) are generally considered as a weak oxidant, they might react with AO7 directly. Ryu and Choi [39] also recently confirmed that $O_2^{\bullet -}$ was mainly responsible for the oxidation of As by photocatalysis. The k in the presence of $O_2^{\bullet -}$ quencher was only 6.2% of the k in the absence. The oxidative species in solution in the presence of $O_2^{\bullet -}$ quencher were mainly O_3 and $HO^\bullet$ from the decomposition of O_3. That is, 6.2% decolorization of AO7 was achieved by O_3 and $HO^\bullet$ from the decomposition of O_3. The contribution of O_3 to the decolorization of AO7 by direct oxidation was 1.5% because the contribution of $HO^\bullet$ from the decomposition of O_3 was 4.7% as discussed above.

4. Conclusion

MWL had excellent performance on decolorazition and mineralization of AO7. Complete decolorization and mineralization were achieved at 80 and 150 min, respectively. Sulfonate groups were completely transformed into SO_4^{2-} and azo-linkages were transformed into N_2, NH_3, NH_4^+ and NO_3^-. The better performance on mineralization of AO7 solution under MWL irradiation than that under conventional electrode lamp irradiation was caused by the synergic effect of UV–vis light and microwave. A large mount of H_2O_2 and O_3 could be generated in AO7 solution under MWL irradiation. These H_2O_2 and O_3 could produce lots of $HO^\bullet$ radicals by decomposition under light irradiation to degrade AO7 dyes effectively.

Acknowledgements

The authors appreciate the generous financial support of this work by the Chinese found 863 project (2002AA601300) and thank to Wuhan University of Science & Engineering for their help in the experiment.

References

[1] S. Kataoka, D.T. Tompkins, W.A. Zelter, M.A. Anderson, J. Photochem. Photobiol. A: Chem. 148 (2002) 323–330.
[2] S. Caddick, Tetrahedron 51 (1995) 10403–10432.
[3] S. Horikoshi, H. Hidaka, N. Serpone, Environ. Sci. Technol. 36 (2002) 1357–1366.
[4] V. Círka, M. Hájek, J. Photochem. Photobiol. A: Chem. 123 (1999) 21–23.
[5] D.H. Han, S.Y. Cha, H.Y. Yang, Water Res. 38 (2004) 2782–2790.
[6] S. Horihoshi, H. Hidaka, N. Serpone, J. Photochem. Photobiol. A: Chem. 153 (2002) 185–189.
[7] S. Horihoshi, H. Hidaka, N. Serpone, Environ. Sci. Technol. 36 (2002) 5229–5237.
[8] S. Horihoshi, H. Hidaka, N. Serpone, J. Photochem. Photobiol. A: Chem. 159 (2003) 289–300.
[9] S. Horihoshi, A. Saitou, H. Hidaka, N. Serpone, Environ. Sci. Technol. 37 (2003) 5813–5822.
[10] S. Horihoshi, H. Hidaka, N. Serpone, J. Photochem. Photobiol. A: Chem. 161 (2004) 221–225.
[11] S. Horihoshi, A. Tokunaga, H. Hidaka, N. Serpone, J Photochem. Photobiol. A: Chem. 162 (2004) 33–42.
[12] P. Klán, J. Literák, M. Hájek, J. Photochem. Photobiol. A: Chem. 128 (1999) 145–149.
[13] J. Literák, P. Klán, J. Photochem. Photobiol. A: Chem. 137 (2000) 29–35.
[14] P. Müller, P. Klán, V. Církva, J. Photochem. Photobiol. A: Chem. 158 (2003) 29–35.
[15] A. Bianco-Prevot, C. Baiocchi, M.C. Brussino, E. Pramauro, P. Savarino, V. Augugliaro, G. Marci, L. Palmisano, Environ. Sci. Technol. 35 (2001) 971–976.
[16] B. Neppolian, H.C. Choi, S. Sakthivel, B. Arabindoo, V. Murugesan, Chemosphere 46 (2002) 1173–1181.
[17] Y. Xu, Chemosphere 43 (2001) 1103–1107.
[18] J. Bandara, J. Kiwi, New J. Chem. 23 (1999) 717–724.
[19] M. Muruganadham, M. Swaminathan, Dyes Pigments 63 (2004) 315–321.
[20] M.A. Behnajady, N. Modirshahla, Chemosphere 55 (2004) 129–134.
[21] A.M. Ei-Dein, J.A. Libra, U. Wiesmann, Chempsphere 52 (2003) 1069–1077.
[22] X. Zhang, Y. Wang, G. Li, J. Mol. Catal. A: Chem. 237 (2005) 199–205.
[23] X. Zhang, Y. Wang, J. Hazard. Mater., in press.
[24] M. Strylidi, D. Kondarides, X. Verykios, Appl. Catal. B: Environ. 47 (2004) 189–201.
[25] Y. Chen, S. Yang, K. Wang, L. Lou, J. Photochem. Photobiol. A: Chem. 172 (2005) 47–54.
[26] S. Malato, J. Blanco, J. caceres, A.R. Fernández-Alba, A. Agüera, A. Rodríguez, Catal. Today 76 (2002) 209–220.
[27] M. Strylidi, D. Kondarides, X. Verykios, Appl. Catal. B: Environ. 40 (2003) 271–286.
[28] F. Wu, N. Deng, H. Hua, Chemosphere 41 (2000) 1233–1238.
[29] G. Low, S. Mcevoy, R. Matthews, Environ. Sci. Technol. 25 (1991) 460–467.
[30] R.L. Ziolli, W.F. Jardim, J. Photochem. Photobiol. A: Chem. 147 (2002) 205–212.
[31] T. Wu, G. Liu, J. Zhao, H. Hidaka, N. Serpone, J. Phys. Chem. B 103 (1999) 4862–4867.
[32] E. Pelizzetti, C. Minero, Colloids Surf. A: Physicochem. Eng. Aspects 151 (1999) 321.C–327.C.
[33] C.C. Wong, W. Chu, Environ. Sci. Technol. 37 (2003) 2310–2316.
[34] D.D. Dionysiou, M.T. Suidan, E. Bekou, I. Baudin, J.M. Laîné, Appl. Catal. B: Environ. 26 (2000) 153–157.

[35] W. Cooper, R. Zlka, R. Petasne, J. Plane, Environ. Sci. Technol. 22 (1988) 1156–1160.

[36] N. Deng, F. Wu, Environmental Photochemistry, Chemistry Industry Publishing Company, Beijing, 2003.

[37] J.C. Zhao, T.X. Wu, K. Wu, K. Oikawa, H. Hidaka, N. Serpone, Environ. Sci. Technol. 32 (1998) 2394–2400.

[38] P. Zhang, F. Liang, G. Yu, Q. Chen, W. Zhu, J. Photochem. Photobiol. A: Chem. 156 (2003) 189–194.

[39] J. Ryu, W.Y. Choi, Effects of TiO_2 surface modifications on photocatalytic oxidation of arsenite: the role of superoxide, Environ. Sci. Technol. 38 (2004) 2928–2933.